



Published in final edited form as:

J Biophotonics. 2021 February ; 14(2): e202000341. doi:10.1002/jbio.202000341.

Harnessing DNA for Nanothermometry.

Graham Spicer^{1,2}, **Sylvia Gutierrez-Erlandsson**³, **Ruth Matesanz**⁴, **Hugo Bernard**⁵,
Alejandro Adam⁶, **Alejo Efeyan**^{#5,*}, **Sebastian Thompson**^{#7,8,*}

¹Wellman Center for Photomedicine, Massachusetts General Hospital, 02114 Boston, MA, USA

²Harvard Medical School, Harvard University, 02115 Boston, MA, USA

³Centro Nacional de Biotecnología, 28049 Madrid, Spain

⁴Centro de Investigaciones Biológicas Margarita Salas 28040, Madrid, Spain

⁵Centro Nacional de Investigaciones Oncológicas (CNIO), 28029 Madrid Spain

⁶Department of Molecular and Cellular Physiology and Department of Ophthalmology, Albany Medical Center, Albany, 12208 NY, USA

⁷Madrid Institute for Advanced Studies in Nanoscience (IMDEA Nanociencia), C/Faraday 9, Madrid 28049, Spain

⁸Nanobiotechnology Unit Associated to the National Center for Biotechnology (CNB-CSIC-IMDEA), Madrid 28049, Spain

These authors contributed equally to this work.

Abstract

Temperature measurement at the nanoscale has brought insight to a wide array of research interests in modern chemistry, physics, and biology. These measurements have been enabled by the advent of nanothermometers, which relay nanoscale temperature information through the analysis of their intrinsic photophysical behavior. In the past decade, several nanothermometers have been developed including dyes, nanodiamonds, fluorescent proteins, nucleotides, and nanoparticles. However, temperature measurement using intact DNA has not yet been achieved. Here, we present a method to study the temperature sensitivity of the ubiquitous DNA molecule within a physiologic temperature range when complexed with fluorescent dye. We theoretically and experimentally report the temperature sensitivity of the DNA-Hoechst 33342 complex in

*Correspondence: Sebastian Thompson, Fundación IMDEA nanociencias, 28049 Madrid Spain, sebastian.thompson@imdea.org; Alejo Efeyan, Centro Nacional de Investigaciones Oncológicas (CNIO), 28029 Madrid Spain, aefeyan@cnio.es.

AUTHOR CONTRIBUTIONS

The manuscript was written through contributions of all authors. All authors have given approval to the final version of the manuscript. G.S. developed the theoretical calculations and analyzed the experimental experiments, R.M. and S.G. performed experiments, A.A. and H.B. designed and analyzed the experimental experiment, A.E. and S.T. develop the concept and supervised the experimental and theoretical experiments.

CONFLICT OF INTEREST

The authors declare no competing financial interest

DATA AVAILABILITY STATEMENT

The data that support the findings of this study are available from the corresponding author upon reasonable request.

SUPPORTING INFORMATION

Additional supporting information is available in the online version of this article at the publisher's website or from the author.

different sizes of double-stranded oligonucleotides and plasmids, showing its potential use as a nanothermometer. These findings allow for extending the thermal study of DNA to several research fields including DNA nanotechnology, optical tweezers, and DNA nanoparticles.

Keywords

Anisotropy; DNA; Hoechst; Nanothermometers; Temperature; thermal information

1 INTRODUCTION

Measuring temperature at nanoscopic scale has attracted much attention in recent years, which is reflected by the increasing number and types of nanothermometers reported^{1–8}. Using these nanothermometers, temperature at the nanoscale has been measured in solution, intracellularly in cancer cells, and in living organisms^{2,5}. These nanothermometers possess the characteristic of changing their photonic properties as a response to changes in intracellular temperature. Among the most important of these properties previously reported are fluorescence intensity⁷, lifetime⁶, anisotropy^{2,5}, fluorescence resonance energy transfer (FRET)⁹, and electron spin in nanodiamonds¹⁰. Anisotropy-based nanothermometers (ABNTs) stand out due to their ability to report temperature in a concentration-independent manner and due to their general compatibility with measurement of biological samples^{2,5,11}. The first report of the ABNT in 2012² measured intracellular temperature of cancer cells using green fluorescent protein (GFP); shortly thereafter, its use expanded to measurement of temperature within living organisms⁵. In the last two years, a method and a practical guide provided the conceptual framework to convert any protein and dye to anisotropy-based nanothermometers^{11,12}. Temperature sensitivity generally increases when the fluorescence lifetime matches the rotational correlation time, dictated by the hydrodynamic radius of the nanothermometer¹². Despite these advances, the use of ABNTs or any other nanothermometers to measure temperature using the intact molecule of DNA remains unexplored. Although the usefulness of DNA for nanothermometry has previously been demonstrated by use of the FRET effect, it required the use of a specially-engineered DNA molecule with tailored secondary structure^{9,13}. This engineered design of DNA for synthesis with FRET dye pairs permitted measurement of temperature from the FRET signal, but the approach is limited to potential applications where DNA can be similarly modified. A more flexible method of extracting temperature information from intrinsic rotational motions in DNA may hold great value in its general applicability. Here we report the thermal sensitivity of endogenous DNA molecules non-covalently bound to Hoechst 33342 dye. Hoechst 33342 is a versatile dye, cell-permeable, innocuous, and can be used for any DNA application since binds to the minor groove at AT-rich regions¹⁴. This sensitivity is herein theoretically described and empirically validated for different sizes of DNA to cover different applications of DNA thermometry. Thus, DNA-based ABNTs constitute an important step towards measurement of temperature in any scientific research field where DNA is used or manipulated.

2 EXPERIMENTAL SECTION

2.1 Sample Preparations

Sample preparations. Hoechst 33342 (Invitrogen) and Fluorescein (Sigma Aldrich) were dissolved in water, whereas GFP (Invitrogen) was dissolved in 1X PBS. Calf thymus DNA (Alfa Aesar) was dissolved at 4 °C overnight in water at a concentration of 10 mg/ml. The solution was then diluted to 1 mg/ml and Hoechst was added at a ratio of 1:100 w/w (Hoechst:DNA), yielding a concentration of 0.01 mg/mL Hoechst. After allowing the mixture to bind for 10 minutes, the solution was then diluted to yield the final solutions of varying concentration. Double-stranded oligonucleotides with the sequences indicated below were purchased from IDT and dissolved in water at a concentration of 10 mg/ml and then diluted in 1X PBS to their final concentrations for testing. The plasmid was linearized by NdeI enzyme treatment following standard protocols.

16 bps: 5GACGGCTGGCTGCTCG3'

32 bps: 5GACGGCTGGCTGCTCGGACGGCTGGCTGCTCG3'

64 bps:

5GACGGCTGGCTGCTCGGACGGCTGGCTGCTCGGACGGCTGGCTGCTCGGACGGCTGGCTGCTCG3'.

Plasmid: pGEMTe-RagC 4 kbps circular plasmid.

2.2 Temperature sensitivity measurements

For temperature sensitivity measurements in solution, a calibration curve relating fluorescence polarization anisotropy (FPA) to temperature was measured using a Horiba Fluorolog fluorometer running in T-format mode with vertically polarized excitation. The temperature sensitivity of each channel was corrected with horizontally polarized excitation. For each experiment, excitation and emission slits were selected to obtain around 10^6 counts per seconds (cps). All samples were measured using a quartz cuvette. Excitation and emission monochromators were set at 350 nm and 450 nm, respectively.

3 RESULTS AND DISCUSSION

3.1 Hoechst as a nanothermometer in solution

We recently reported the specific requirements for protein-dye complexes to be used as ABNTs based on a theoretical model^{11,12} and showed that dyes such as Hoechst, with a fluorescence lifetime lower than 1 ns, provide adequate temperature sensitivity in their unbound state¹². Thus, dyes with this property are useful for nanothermometry and can be used to measure temperature at the nanoscale without further modification. In the case of Hoechst 33342 (unbound fluorescence lifetime of around 0.35 ns¹⁵), this dye is expected to have a temperature sensitivity of -2.4 milliunit (mU) of anisotropy per K¹². To experimentally test this theoretical prediction, we compared the temperature sensitivity of Hoechst in water to the sensitivity of fluorescein in water and of GFP in PBS. Fluorescein and GFP have been selected as controls because their fluorescence anisotropy-based

temperature sensitivity has been previously reported^{2,11}. The temperature sensitivities of these three dye-based nanothermometers are shown in Figure SI 1. Likewise, their theoretical¹² and experimental sensitivities are compared in table 1.

Experimental temperature sensitivities for these three fluorochromes fit from the plots in Figure SI 1 are fully consistent with their theoretically predicted sensitivities, as can be appreciated in Table 1. These results also indicate that Hoechst (and in principle, all other free dyes with fluorescence lifetimes below 1 ns such as DAPI, Cy3, and Indocyanine Green) can be used in their unbound form as ABNTs.

3.2 DNA-Hoechst as nanothermometer

Hoechst is routinely used to stain double-stranded DNA. Three types of Hoechst dye are routinely used: Hoechst 33258, Hoechst 33342, and Hoechst 34580. For this study, we selected Hoechst 33342 since it is the one typically preferred for biological experiments. We sought to determine the temperature sensitivity of Hoechst 33342 dye when bound to DNA, and to evaluate the potential of the DNA-Hoechst ABNT for temperature measurement. Hoechst binds to the minor groove of DNA at AT-rich regions¹⁴. In addition to largely increasing fluorescence intensity, once Hoechst is conjugated with DNA, its fluorescence lifetime increases from 0.35 ns to 2.2 ns¹⁶. This change, however, does not theoretically limit the use of the DNA-Hoechst complex as an ABNT since the hydrodynamic radius will also increase. Thus, we studied the temperature sensitivity of this complex formed with DNA molecules across a broad range of base-pair (bp) lengths (16 bps oligonucleotides, 32 bps oligonucleotides, 64 bps oligonucleotides, 4 kilobase pairs (kbps) DNA fragments and 16 kbps calf thymus DNA fragments). The schematic representation of DNA-based ABNT synthesis is illustrated in Figure 1(a) and the experimental data are shown in Figure 1(b–f).

These results show DNA length and temperature sensitivity are inversely correlated plateauing at 0.5×10^{-3} mU per K for the DNA fragments with lengths of 64 bps, 4 kbps and 16 kbps. Likewise, ABNTs made from short DNA (16 bps and 32 bps) present higher temperature sensitivity values compared with those made from long DNA. The highest temperature sensitivity was achieved from short DNA oligonucleotide-based ABNTs with a length of 16 bps, due to the match between the dye's fluorescence lifetime and the rotational correlation time of the DNA-Hoechst complex. To theoretically support this experimental observation, we directly applied the previously derived model for ABNT sensitivity to the DNA-Hoechst complex. However, previous work on ABNTs (fluorescent proteins, dyes, or protein-dye complexes^{2,5,11,12}) defined a rotationally isotropic system where the rotational correlation time Θ_R of the molecule is governed by its spherical hydrodynamic volume V (or hydrodynamic radius) and the shear viscosity of the pure solvent $\eta(T)$; this can be expressed by the Stokes-Einstein-Debye relation

$$\Theta_R = \frac{V\eta(T)}{kT} \quad (1)$$

Where k is Boltzmann's constant and T is temperature. This relationship holds for the domain where solvent viscosity is independent of solute concentration and the

hydrodynamic volume is known; in principle this is reserved for molecules with spherical rotational symmetry. For ABNTs with hydrodynamic properties that fall within this regime, the sensitivity has been defined by the following equation¹¹:

$$S = -r_0 \cdot \frac{\frac{k\tau_f}{V\eta(T_0)}\left(1 + \frac{B}{T_0}\right)}{\left(1 + \frac{k\tau_f T_0}{V\eta(T_0)}\right)^2} \quad (2)$$

Where r_0 is a delimiting FPA, k is Boltzmann's constant, τ_f is fluorescence lifetime, V is the hydrodynamic volume, $\eta(T_0)$ is the dynamic viscosity at the reference temperature, T_0 and B is a constant of the Arrhenius expression for dynamic viscosity. When considering the sensitivity of aqueous solutions of dilute dyes or proteins, the dynamic viscosity is the only important parameter of the surrounding solvent that influences ABNT sensitivity.

3.3 Theoretical studies of DNA-Hoechst as a nanothermometer

To apply this model to DNA-based ABNTs, additional variables must be taken into account because DNA-based ABNTs present different geometric and hydrodynamic properties, as compared to spherical proteins:

- *Rotational motion*: DNA presents different rotational motion than a molecule with spherical symmetry. To understand molecular motion of DNA fragments, different physical models for different DNA lengths should be considered: oligonucleotides shorter than 150 bps can be approximated as short rigid rods in solution¹⁷, where molecular motion is encompassed by rotation orthogonal to the rod's axis (tumbling of the rod), and rotation around the rod's axis¹⁷. The aspect ratio of a rod-like molecule, p , defined as its length divided by diameter $p \equiv \frac{L}{d}$, determines the equivalent hydrodynamic radius of rotation in solution resulting in an adjusted rotational correlation time for rigid rodlike molecules Θ_{RR} :

$$\Theta_{RR} = \frac{\pi L^3 \eta(T)}{3kT \cdot (\ln(p) + \delta)}$$

Alternatively, this can be expressed as the rotational diffusion coefficient for spherical macromolecules multiplied by a scaling factor S for rod-like molecules, where

$$S = \frac{1}{2}(3(\ln(p) + \delta))^{-\frac{1}{3}}$$

and δ represents a correction for end effects of the rod in solution. Taking this correction into account, the theoretical sensitivity for rigid rod-shaped oligonucleotide based ABNTs can be predicted as a function of their length in base pairs, shown in Figure 2 and the practical values in table 2

The measured temperature sensitivity of almost all samples differ significantly compared with the theoretically predicted values presented in table 2. Most notably, and contrary to the

theoretical prediction, the fluorescence anisotropy of the dye bound to large DNA fragments also shows temperature sensitivity. To understand these differences between the theoretical predictions and the experimental values, several other geometric and hydrodynamic properties for both the DNA and Hoechst should be considered and described:

- *Torsional and bending motions (DNA)*: When considering modes of motion in longer fragments of DNA, twisting and bending of the chain macromolecule cannot be neglected. The model of rotation, twisting, and bending of the semiflexible DNA helix presented by Barkley and Zimm¹⁸ treats this Brownian phenomenon with analytical rigor. Further study of relevant physical constants behind torsional and bending rigidity of DNA¹⁹ inform our analysis of the effects of these motions on potential temperature sensitivity of DNA-based nanothermometers. Figure 3 presents the magnitude of FPA temperature sensitivity evaluated at 37 °C for a 2.2 ns lifetime dye, evaluated using the Barkley-Zimm model, plotted along with the experimental data.

It is apparent that temperature sensitivity decays rapidly for long DNA chains when the additional modes of torsional and bending motion in the semiflexible DNA model are considered. As can be appreciated in Figure 4, these motions fail to explain the temperature sensitivity observed in larger DNA-based ABNTs.

Since the aforementioned DNA motions fail to provide a suitable explanation for the remaining temperature sensitivity in longer DNA to explain the experimental temperature sensitivity, additional sources of dye motion must be considered:

- *Dye wobbling*: Another potentially relevant mode of motion is the wobbling of the non-covalently bound dye within the DNA groove²⁰. This motion should affect any DNA length, and its magnitude is independent of DNA length. Wobbling plays a fundamental role in the depolarization of fluorescent light and thus in the anisotropy signal¹⁹. While the correlational time of dye wobbling has been studied for ethidium bromide, its relative influence remains unclear for other dyes such as Hoechst. Specifically, while the cone-like wobbling correlation time was reported to be on the order of 80–250 ns which would be too long to significantly affect FPA²⁰, other independent dye motions with correlation times on the order of 0.1 ns have been found to contribute to anisotropy decay²¹. Since other DNA motions cannot be responsible for FPA-based temperature sensitivity in long DNA-based ABNTs, we assume that independent wobbling of the dye may play a role in the light depolarization. Consequently, the following scenario is hypothesized for DNA-Hoechst complexes. Fluorescence anisotropy (and its sensitivity to temperature) of the DNA-Hoechst complex will depend not only on the hydrodynamic radius of the complex, but on two different motions: (1) rotational motion and (2) wobbling of the dye about the intercalated site of binding²⁰. It should be mentioned that Brownian dynamics of DNA molecules also present bending motions. For the experimental conditions of the analysis of short nucleotide lengths, the effects of DNA bending on FPA can be considered as negligible when compared with other types of motion^{18,20}.

Considering these new variables, we can analyze now the experimental data obtained in Fig 2. For example, in the case of the 16 bps DNA oligonucleotide, the sensitivity was expected

to be around -2.5 mU per K and was measured to be around -1.2 mU per K. In this case, we believe that both movements influence the depolarization of the light: rotational motions of the DNA-Hoechst complex and the independent conical wobbling of the dye about its bond to the DNA. For longer chains (exceeding 150 bps), sensitivity was predicted to be zero only if torsional and bending motion governs the depolarization of the fluorescence. The complex presents a rotational correlation time that has a minimal effect on fluorescence anisotropy behavior and thus temperature sensitivity. We believe that the movement that governs the fluorescence depolarization is mainly due to the wobbling of the dye bound to the DNA minor groove. This motion causes the temperature sensitivity of -0.5 mU per K; this value is not the highest sensitivity that can be achieved using ABNTs. However, by using dyes with different fluorescence lifetimes, the sensitivity can be improved.

In brief, our data are consistent with the theoretical calculations in the following: (1) the movement that governs the anisotropy signal from short DNA oligonucleotides is a combination of dye wobbling and the rotational motion of the DNA; (2) the anisotropy signal from long DNA molecules is dominated by the wobbling of the dye.

3.4 Temperature sensitivity in circular DNA

To lend experimental support to this statement, we compared the temperature sensitivity of a DNA-based ABNT formed by a 4 kbps circular plasmid against the same plasmid (same sequence and length) previously linearized by NdeI enzyme. In circular DNA, rotational motions about the principal chain axis are not possible, in contrast to this motion in linearized DNA. However, both linear and circular forms will have the same degree of dye wobbling. Results can be observed in Figure 4:

As can be appreciated, the same temperature sensitivity is measured in linear and circular DNA of the same sequence and length. This shows that the temperature sensitivity found in longer DNA fragments is not due to rotational motion of DNA, and instead is presumably governed by the characteristic rate of wobbling of the dye bound to the DNA.

Finally, we considered the effect of the solution viscosity, a key parameter governing the temperature sensitivity of ABNTs. Likewise, the concentration of DNA in solution also effects the overall viscosity and will likely influence the temperature sensitivity of ABNTs:

- *Solution viscosity*: Previous ABNT studies neglected intermolecular forces between solute molecules that affect the rotation of ABNTs in solution (viscosity). For DNA, consideration for solutions of oligonucleotides is the effect of solute molecule concentration on the solution viscosity. For short DNA molecules, the concentration of DNA affects bulk solution viscosity and subsequent rotational diffusion and correlation times of DNA-based ABNTs. In the dilute regime, where forces between solute molecules are negligible, the solution viscosity η_S follows a linear relationship with nucleotide concentration, C , following Newtonian behavior²². As concentration increases, the polymer chains overlap at a characteristic concentration, C^* . The characteristic overlap concentration C^* , represents a threshold above which there is a deviation from the Newtonian regime of dilute solutions, depending solely on the polymer solute molecular weight W and molecular radius of

gyration $S: C^* \propto W \cdot S^{23}$. For nucleic acids with lengths on the order of 11–45 kbps, experimentally-derived values of C^* range from 0.09 – 0.03 mg/mL, dependent on the quality of the solvent which influences the radius of gyration of the DNA in solution²². In nucleic acids exceeding several kbps, the hydrodynamic behavior is better modeled according to polymer chain dynamics. When concentration increases, a second critical concentration is reached, the entanglement concentration, C^{**} . This concentration represents a polymer solution with uniform entanglement interactions between solute molecules^{24–26}. For long DNA molecules, the extent of the dilute regime, where viscosity scales linearly with nucleic acid concentration, remains independent of solution temperature. The solution viscosity, therefore, can be considered as a function of temperature and solute concentration as independent variables $\eta(T,C)$ in equation (1). However, this limitation is strongly dependent on the desired solvent, so we recommend testing experimentally the temperature sensitivity for other solvents. Thus, this reduced robustness of FPA temperature sensitivity at high macromolecular concentrations should not represent a limit in the use of DNA-based ABNTs for many nanotechnology applications or biological applications. FPA values as a function of temperature for different DNA concentrations and buffer solutions are shown in Supplementary Information (SI Fig 2, SI Fig 3, and SI Fig 4). While deviations in the relationship between fluorescence anisotropy and temperature are evident, and presumably due to several competing effects, this relationship remains strong for dilute samples, indicating that temperature measurement using the DNA molecule is possible.

4 CONCLUSIONS

In conclusion, we have elucidated three important rules governing and allowing thermometry at the nanoscale. First, we gathered robust experimental support for the universal utility of dyes with fluorescence lifetime lower than 1 ns for nanothermometry. This advance allows the addition of temperature measurement to multiple techniques and experiments without the need to introduce additional nanothermometers or other molecular probes to the system under study. Second, we present theoretical and experimental temperature measurements at the nanoscale using several different types of DNA as nanothermometers. Finally, we found that large DNA molecules labeled with Hoechst display a degree of temperature sensitivity based on the wobbling of the dye about its bond to the DNA. These findings enable the extension of temperature measurement to any research areas that study DNA or utilize DNA as, for example, a template, nanoparticle, or for gene transfection. In summary, we have developed a method to obtain precise temperature information utilizing the DNA molecule.

Supplementary Material

Refer to Web version on PubMed Central for supplementary material.

ACKNOWLEDGMENTS

S.T. dedicates this manuscript in the memory of his PhD mentor Professor C.M. Drain. This work was supported by RETOS RTI2018-101050-J-I00 (ST), National Institute of General Medical Sciences of the National Institutes of Health under award number R01GM124133 (A.A), Ramon y Cajal Grant (RYC-2013-13546) and by SAF2015-67538-R (MCIU/AEI/FEDER, UE) (AE).

Abbreviations:

ABNTs	anisotropy based nanothermometers
Rh	hydrodynamic radius

REFERENCES

- (1). Baffou G; Girard C; Quidant R Mapping Heat Origin in Plasmonic Structures. *Phys. Rev. Lett* 2010, 104 (13), 1–4.
- (2). Donner JS; Thompson SA; Kreuzer MP; Baffou G; Quidant R Mapping Intracellular Temperature Using Green Fluorescent Protein. *Nano Lett.* 2012, 12 (4), 2107–2111. [PubMed: 22394124]
- (3). Lucia U; Grazzini G; Montrucchio B; Grisolia G; Borchiellini R; Gervino G; Castagnoli C; Ponzetto A; Silvagno F Constructal Thermodynamics Combined with Infrared Experiments to Evaluate Temperature Differences in Cells. *Sci Rep.* 2015 6 23;5:11587 [PubMed: 26100383]
- (4). Vetrone F; Naccache R; Zamarró A; Juarranz A; Fuente D; Sanz-rodri F; Maestro LM; Marti E; Jaque D; Capobianco JA Temperature Sensing Using Fluorescent Nanothermometers. *ACS Nano* 2010, 4 (6), 3254–3258. [PubMed: 20441184]
- (5). Donner JS; Thompson SA; Alonso-Ortega C; Morales J; Rico LG; Santos SICO; Quidant R Imaging of Plasmonic Heating in a Living Organism. *ACS Nano* 2013, 7 (10), 8666–8672. [PubMed: 24047507]
- (6). Okabe K; Inada N; Gota C; Harada Y; Funatsu T; Uchiyama S Intracellular Temperature Mapping with a Fluorescent Polymeric Thermometer and Fluorescence Lifetime Imaging Microscopy. *Nat. Commun* 2012, 3, 705. [PubMed: 22426226]
- (7). Savchuk OA; Silvestre OF; Adão RMR; Nieder JB GFP Fluorescence Peak Fraction Analysis Based Nanothermometer for the Assessment of Exothermal Mitochondria Activity in Live Cells. 2019, No. April, 1–11.
- (8). Bradac C; Lim SF; Chang H; Aharonovich I Optical Nanoscale Thermometry : From Fundamental Mechanisms to Emerging Practical Applications. 2020, 2000183, 1–29.
- (9). Gareau D; Laurent A; Desrosiers T; Vallée-bélisle A Programmable, Quantitative, DNA Nanothermometers. *Nano Lett.* 2016, 16 (7), 3976–3981. [PubMed: 27058370]
- (10). Glushkov E; Navikas V; Radenovic A Fluorescent Nanodiamonds as Versatile Intracellular Temperature Sensors. 2019, 73 (1), 73–77.
- (11). Thompson SA; Martinez IA; González PH-; Adam A; Jaque D; Nieder JB; De. Rica R Plug and Play Anisotropy-Based Nanothermometers. 2018.
- (12). Spicer G; Efeyan A; Adam AP; Thompson SA Universal Guidelines for the Conversion of Proteins and Dyes into Functional Nanothermometers. 2019, No. April, 1–9.
- (13). Youshen Wu, Jiajun Liu, Ya Wang, Ke Li, Lei Li, Jianhua Xu, W. D Novel Ratiometric Fluorescent Nanothermometers Based on Fluorophores-Labeled Short Single-Stranded. *ACS Appl. Mater. Interfaces* 2017, 9 (12), 11073–11081. [PubMed: 28263548]
- (14). Bucevi ius J; Lukinavi ius G; Gerasimaite R The Use of Hoechst Dyes for DNA Staining and Beyond. *Chemosensors* 2018, 6 (2).
- (15). Vekshin N Binding of Hoechst with Nucleic Acids Using Fluorescence Spectroscopy. *J. Biophys. Chem* 2011, 02 (04), 443–447.
- (16). Baggaley E; Botchway SW; Haycock JW; Morris H; Sazanovich IV; Williams JAG; Weinstein JA Long-Lived Metal Complexes Open up Microsecond Lifetime Imaging Microscopy under Multiphoton Excitation: From FLIM to PLIM and Beyond. *Chem. Sci* 2014, 5 (3), 879–886.
- (17). Goodman A; Tseng Y; Wirtz D Effect of Length, Topology, and Concentration on the Microviscosity and Microheterogeneity of DNA Solutions. 2002, 2836 (02), 199–215.
- (18). Barkley MD; Zimm BH Theory of Twisting and Bending of Chain Macromolecules; Analysis of the Fluorescence Depolarization of DNA. *J. Chem. Phys* 1979, 70 (6), 2991–3007.

- (19). Millar DP; Robbins RJ; Zewail AH Torsion and Bending of Nucleic Acids Studied by Ultrashort Time-Resolved Fluorescence Depolarization of Intercalated Dyes. *J. Chem. Phys.* 1982, 76 (4), 2080–2094.
- (20). Hard T; Kearns R, D. Anisotropic Overall and Internal Motions of Short DNA Fragments. *Nucleic Acids Res.* 1986, 14 (9), 3945–3956. [PubMed: 3714500]
- (21). Magde D; Zappala M; Knox WH; Nordlund TM Picosecond Fluorescence Anisotropy Decay in the Ethidium/DNA Complex. *J. Phys. Chem* 1983, 87 (17), 3286–3288.
- (22). Pan S; At Nguyen D; Sridhar T; Sunthar P; Ravi Prakash J Universal Solvent Quality Crossover of the Zero Shear Rate Viscosity of Semidilute DNA Solutions. *J. Rheol. (N. Y. N. Y)* 2014, 58 (2), 339–368.
- (23). Graessley WW Polymer Chain Dimensions and the Dependence of Viscoelastic Properties on Concentration, Molecular Weight and Solvent Power. *Polymer (Guildf).* 1980, 21 (3), 258–262.
- (24). Raspud E; Lairez D; Adam M On the Number of Blobs per Entanglement in Semidilute and Good Solvent Solution: Melt Influence. *Macromolecules* 1995, 28 (4), 927–933.
- (25). Odijk T Possible Scaling Relations for Semidilute Polyelectrolyte Solutions. *Macromolecules* 1979, 12 (4), 688–693.
- (26). Mason TG; Dhople A; Wirtz D Linear Viscoelastic Moduli of Concentrated DNA Solutions. *Macromolecules* 1998, 31 (11), 3600–3603.

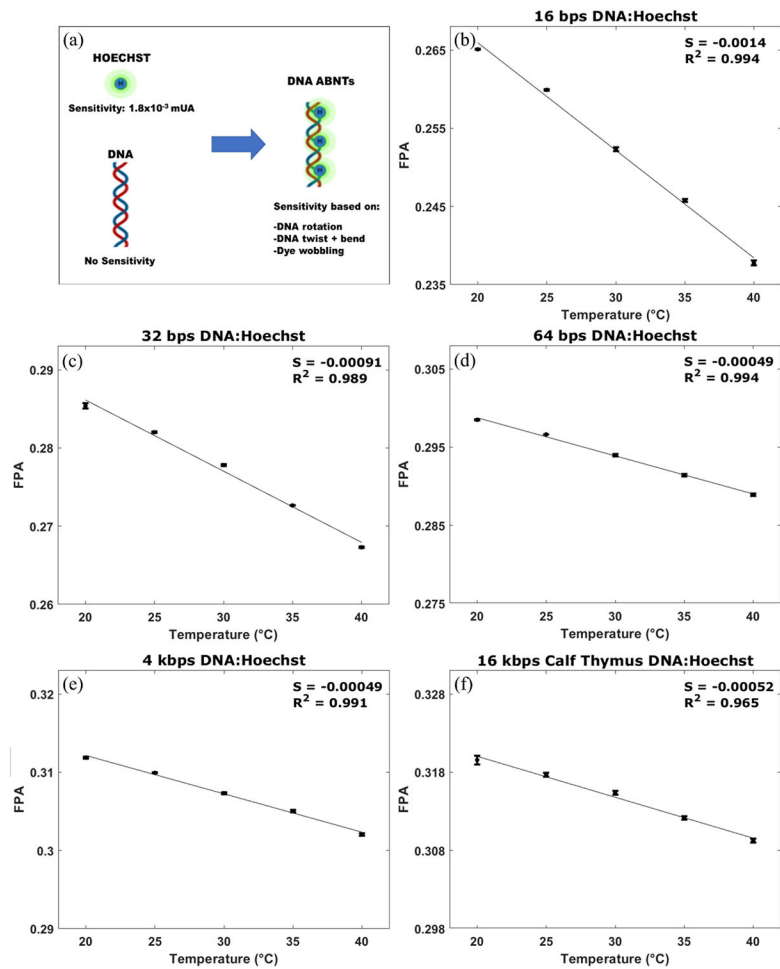


Figure 1.

(a) Schematic illustration of DNA-based ABNT synthesis. (b-f) show the experimental temperature sensitivity of different 0.1 mg/ml (b-e) and 0.01 mg/ml* (f) DNA-based ABNTs (100:1 DNA:HOECHST ratio in grams). Error bars represent the standard error of the mean value. (*) The concentration of 16 kbps DNA-based ABNTs was selected to be 0.01 mg/ml because for DNA fragments longer than 11 kbps, the temperature sensitivity is compromised above concentrations of 0.03 – 0.09 mg/ml (see discussion of viscosity below).

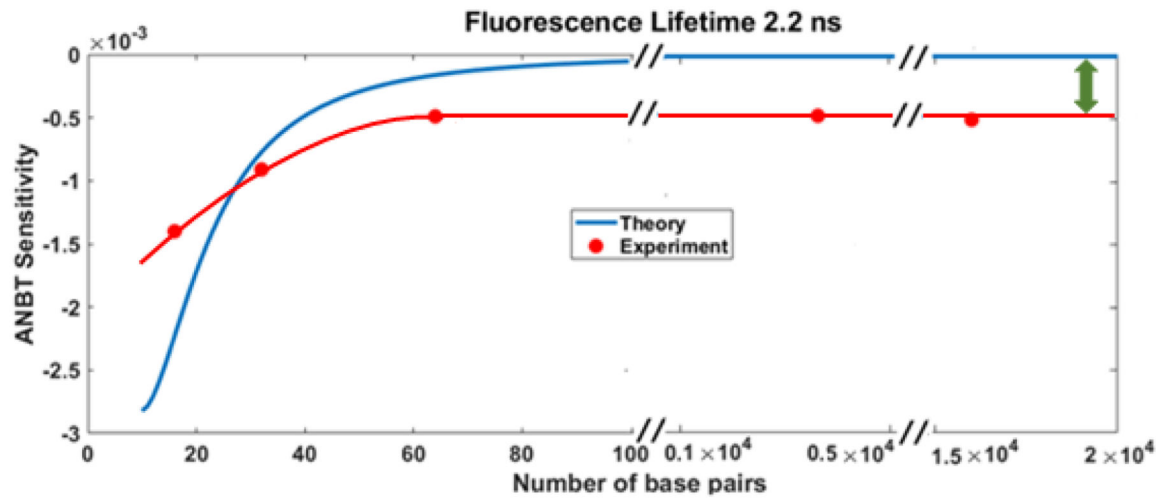


Figure 2.

(a) Theoretical and experimental sensitivity as a function of number of base pairs for oligonucleotide-Hoechst ABNTs (fluorescence lifetime of 2.2 ns). Green arrow shows the deviation from expected temperature sensitivity for long DNA molecules.

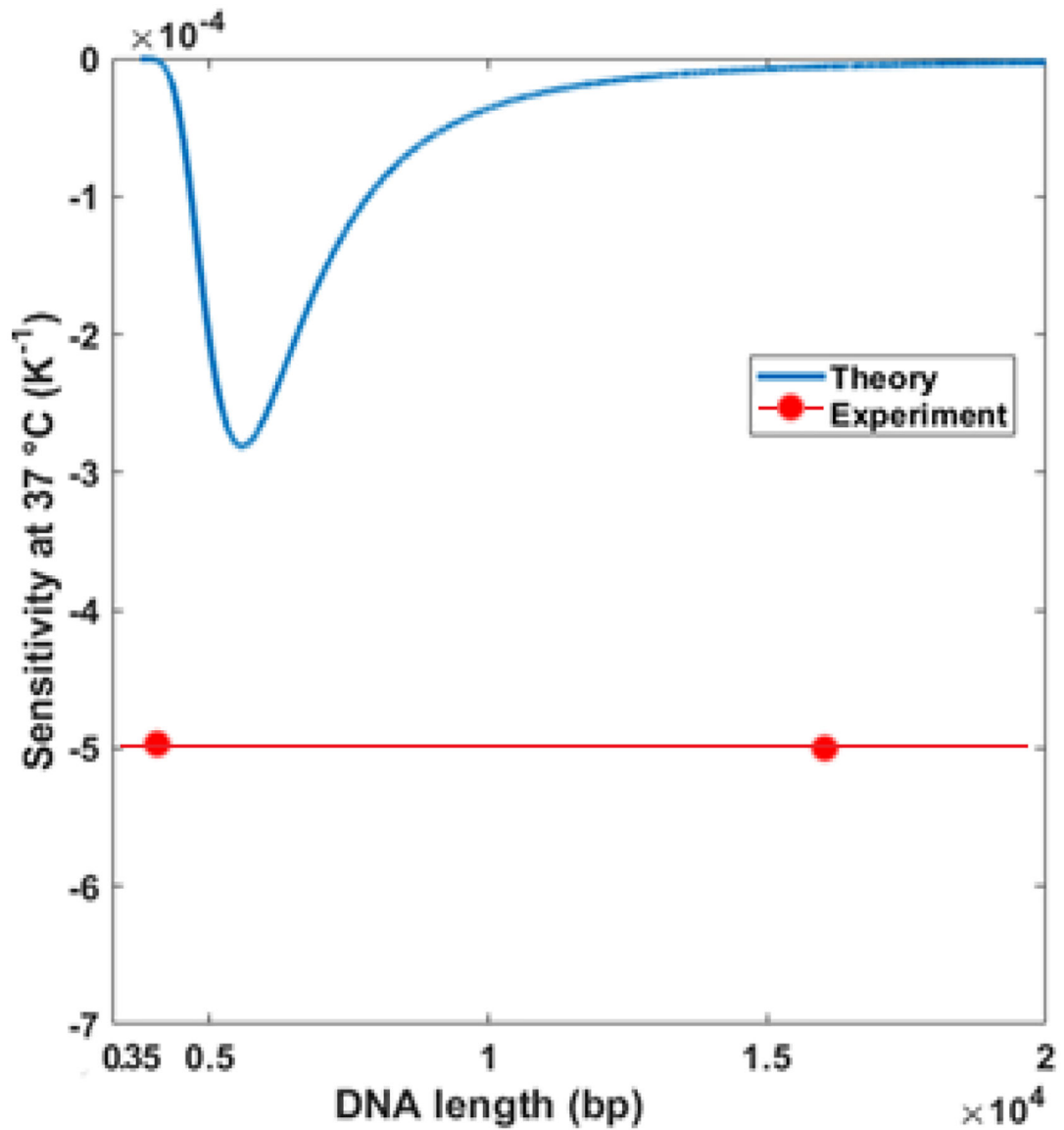


Figure 3. Theoretical DNA-Hoechst ABNT sensitivity evaluated at 37 °C from the Barkley-Zimm model (torsion, rotation, bending motions) with the experimental data.

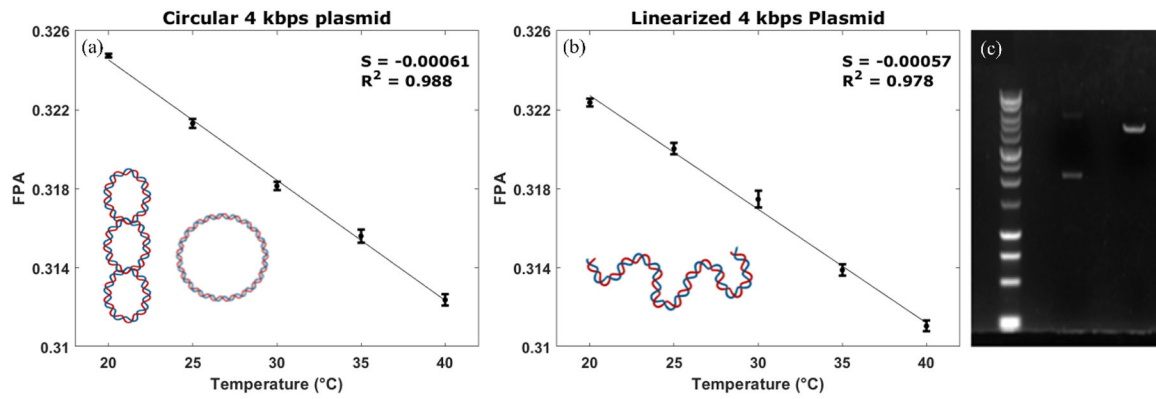


Figure 4.

Temperature sensitivity of the 4 kbps pGEMTe-RagC circular plasmid (a) versus the same linear plasmid (b) after NdeI enzyme treatment (plasmid concentration 0.1 mg/mL, Hoechst concentration 0.001 mg/mL). Error bars represent the standard error of the mean value. Gel electrophoresis (c) showing the circular uncut plasmid (middle row - two bands) and linear conformation (right row - one band).

Table 1.

Theoretical and measured sensitivity values for Hoechst, Fluorescein, and GFP.

Dye	Theoretical Sensitivity ¹² (mU)	Experimental Sensitivity (mU)
GFP	-1.7×10^{-3}	-1.4×10^{-3}
Fluorescein	-0.36×10^{-3}	-0.4×10^{-3}
Hoechst	-2.4×10^{-3}	-1.8×10^{-3}

Author Manuscript

Author Manuscript

Author Manuscript

Author Manuscript

Table 2.

Experimental and theoretical values for DNA-based ABNT sensitivity

DNA-based ABNT	Theoretical (mU)	Experimental (mU)
16 bps	-2.5×10^{-3}	-1.1×10^{-3}
32 bps	-0.7×10^{-3}	-0.8×10^{-3}
64 bps	-0.1×10^{-3}	-0.49×10^{-3}
4 kbps	-1×10^{-12}	-0.49×10^{-3}
16 kbps	-1×10^{-12}	-0.52×10^{-3}

Author Manuscript

Author Manuscript

Author Manuscript

Author Manuscript